Direct observation of conductance fluctuations of a single-atom tunneling contact

A. Sperl, J. Kröger,* and R. Berndt
Institut für Experimentelle und Angewandte Physik, Christian-Albrechts-Universität zu Kiel, D-24098 Kiel, Germany
(Received 28 August 2009; published 7 January 2010)

Using a cryogenic scanning tunneling microscope, the dynamics of lateral translations of a single silver atom adsorbed on Ag(111) were investigated with a time resolution of 10 ns. Elevated tunneling currents passed through the tip close to the adsorbed atom induce sudden adsorption site changes, which are reflected by two-level fluctuations of the tunneling conductance. The voltage dependence of the fluctuation rate reveals different local heating of the adsorbed atom in different positions relative to the tip.

DOI: 10.1103/PhysRevB.81.035406 PACS number(s): 68.37.Ef, 73.40.Jn, 73.63.Rt, 74.40.-n

I. INTRODUCTION

Local heating of atom-sized contacts is vividly discussed since it may have profound influence on future atomic or molecular electronics.[1] Measurements of effective junction temperatures provide insight into the balance between energy dissipation at the single atom or molecule and heat transfer into the contacting electrodes.[2] Such measurements of effective temperatures, however, are difficult due to the lack of appropriate thermometers. Indirect probes for local heating effects have been reported from atomic force and scanning tunneling microscopy (STM). The atomic force microscope was used to measure the force required to break molecule-electrode bonds.[3] Since the bond rupture process is thermally activated, effective temperatures of the molecular junction were extracted as a function of the voltage applied to the junction. With STM conductance-distance curves were acquired on single C_{60} molecules.[4] The width of the transition between tunneling and contact was used to extract an effective temperature. Another indirect probe for effective temperatures is the controlled decomposition of fullerene molecules, which were heated by elevated currents.[5] A more direct method to evaluate effective temperatures of nanometer-scaled junctions is the measurement of two-level fluctuations, which appear in the conductance of such contacts.[6–9] These two-level fluctuations occur when two stable atomic configurations exist and the contact switches between them by thermal activation. Time-resolved measurements of two-level conductance fluctuations with STM are rare. Agraït *et al.*[10] reported conductance switching of Au and Pb contacts resulting from atoms oscillating between tunneling and contact regimes. Stroscio *et al.*[11] investigated conductance fluctuations in the course of single-cobalt manipulation on Cu(111). In these experiments, the switching of Co adsorption sites between hexagonal close-packed (hcp) and face-centered-cubic (fcc) sites was controlled by the tip-surface distance and by the tunneling voltage (V). While for $|V| \leq 5$ mV an almost constant background of the switching rate was observed and explained in terms of voltage-independent quantum tunneling of the Co atom between hcp and fcc sites, a strong increase in the switching rate was reported for $5 \leq |V| \leq 10$ mV. This strong increase was interpreted in terms of a nonthermal population of Co vibration modes excited through inelastic electron tunneling.

Here, we present a study of lateral translation dynamics of a Ag atom adsorbed on Ag(111) with a time resolution of 10 ns and in an extended voltage range between 1 mV and 0.5 V. Positioning the tip off the center of the adsorbed atom (adatom) at elevated tunneling conductances (≈ 0.1 G_0, $G_0 \approx 77.5$ μS: quantum of conductance) induces random transitions between fcc and hcp adsorption sites, which are related to two-level fluctuations of the tunneling conductance. The voltage dependence of these fluctuations was used to extract effective temperatures of the adatom and diffusion barrier heights in the presence of the tip. The effective temperature of the adatom depends on its position relative to the tip and reaches ≈ 20 K at the highest voltage applied. The barrier heights between adsorption sites are drastically lowered due to the presence of the tip and reach several millivolts only.

II. EXPERIMENT

The experiments were performed with a custom-built scanning tunneling microscope operated at 7 K and in ultrahigh vacuum with a base pressure of 10^{-9} Pa. The Ag(111) surface and chemically etched tungsten tips were cleaned by argon-ion bombardment and annealing. Single silver atoms were deposited onto the surface by controlled tip-surface contacts.[12] To acquire time-resolved conductance fluctuations a transimpedance amplifier was used with a 3 dB cutoff frequency of 30 MHz at 100 pF, which is the capacitance of the shielded cable carrying the tunneling current from the tip of the microscope to the amplifier. The experimental setup enables a time resolution of less than 10 ns.

III. RESULTS AND DISCUSSION

Figure 1 illustrates the experimental conditions, at which conductance fluctuations were observed. In Fig. 1(a) the STM image shows a single Ag adatom on Ag(111), which according to calculations occupies fcc substrate sites.[13] A cross indicates the lateral position of the tip above the surface, which is ≈ 1 Å off the adatom center. Placing the tip exactly atop the adatom did not lead to conductance fluctuations. The vertical tip position likewise plays a role for the observation of conductance fluctuations as illustrated in Fig. 1(b), which shows the evolution of the conductance, G, as a function of the tip displacement, Δz. The characteristics of such conductance traces have been discussed in Ref. 14. Here, we use the conductance curve to show that conduc-

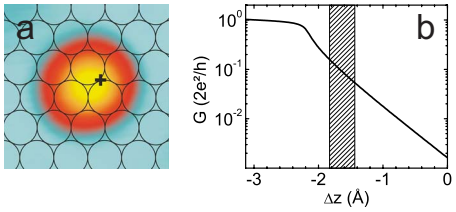

FIG. 1. (Color online) (a) Constant-current STM image of a single Ag atom adsorbed on Ag(111) along with indicated surface lattice (black circles). The cross shows the lateral tip position during time-resolved measurements of the adatom translations (1.4 nm $\times$1.4 nm, 0.1 V, and 0.1 nA). (b) Conductance (G) versus tip displacement (Δz) acquired at the center of the adatom. The conductance curve comprises tunneling ($0>\Delta z>-2$ Å), transition from tunneling to contact ($-2>\Delta z>-2.2$ Å), and contact ($\Delta z<-2.2$ Å). Zero displacement corresponds to feedback loop parameters of 0.1 V and 10 nA. The hatched area shows the conductance range where two-level fluctuations were probed.

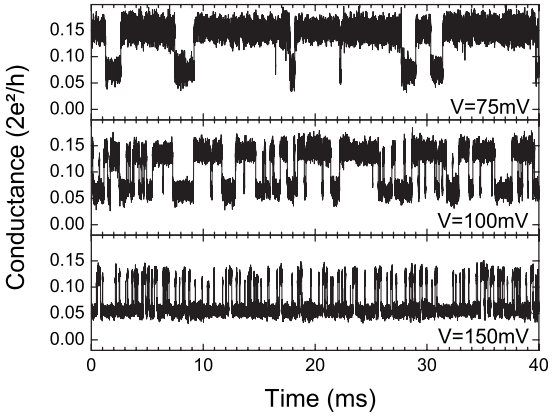

FIG. 2. Two-level fluctuations of the conductance at the indicated voltages and acquired with the tip-adatom configuration shown in Fig. 1(a). The feedback loop was opened at an average conductance of $G\approx 0.1$, G_0. Conductance levels of ≈ 0.15, G_0 and ≈ 0.06, G_0 correspond to the adatom residing at an hcp and fcc site, respectively.

tance fluctuations started to occur for conductances exceeding 0.05 G_0, which still belong to the tunneling regime. This conductance is in good agreement with the threshold conductance for moving single Ag adatoms on Ag(111) using the tip of a scanning tunneling microscope.[15] For different adsorbate-substrate combinations the tunnelling parameters for tip-assisted single-atom or single-molecule translations vary.[16,17] In particular, the conductance fluctuations to be discussed next are most likely due to lateral motions of the adatom. Vertical adatom movements would lead to closing and opening of the tunneling gap between tip and adatom and would involve single-adatom conductances of ≈ 1 G_0.[12] As soon as the tip-adatom spacing was small enough to observe two-level fluctuations of the conductance with a similar mean time spent in each level then the tip-surface distance was frozen by opening the STM feedback loop and the sample voltage was varied to explore the voltage dependence of the fluctuation rate.

Typical time-resolved two-level fluctuations are presented in Fig. 2. At the indicated voltages the conductance displays fluctuations between ≈ 0.06 G_0 and ≈ 0.15 G_0. According to the tip position introduced in Fig. 1(a), the high conductance level corresponds to the adatom residing at the hcp site, since in this case the tip-adatom distance is smaller than for the adatom residing at the fcc site. The observation of only two conductance levels indicates that the total potential resulting from the periodic lattice potential and the attractive tip potential exhibits two minima, namely one at the fcc and the other at the hcp site closest to the tip. Figure 2 shows two trends with increasing voltage: first, the fluctuation rate increases and, second, the average occupation time of the hcp site ($\bar{\tau}_{\mathrm{hcp}}$) decreases in favor of an increasing average occupation time of the fcc site ($\bar{\tau}_{\mathrm{fcc}}$). For instance, at 75 mV, $\bar{\tau}_{\mathrm{hcp}}>\bar{\tau}_{\mathrm{fcc}}$, while at 100 mV, $\bar{\tau}_{\mathrm{hcp}}\approx\bar{\tau}_{\mathrm{fcc}}$, and at 150 mV, $\bar{\tau}_{\mathrm{hcp}}<\bar{\tau}_{\mathrm{fcc}}$. Consequently, for small voltages the adatom preferentially occupies the hcp site, which is closer to the tip apex. Using a transimpedance amplifier with too low a cutoff frequency, the increasing conductance fluctuation rate with increasing voltage could be interpreted as negative differential conductance. As shown in Fig. 2 the average conductance value for 75 mV is higher than for 100 and 150 mV. We further note that for $|V|<1$ mV two-level fluctuations occurred with a rate of less than 0.2 s^{-1}, which is most likely due to Ag adatom tunneling between hcp and fcc sites. For Co atoms on Cu(111) a tunneling rate between 1 and 20 s^{-1} was reported.[11]

Two-level conductance fluctuations are random in nature and a model that describes these fluctuations must take the stochastic behavior into account. In particular, the question arises how to define a reasonable mean residence time for hcp and fcc sites based on the measured time series of random conductance fluctuations. Conductance fluctuations have previously been considered as Markov processes,[11] in which two subsequent events occur independently from each other. The probability, P_i, (i=hcp,fcc), that a fluctuation from level i occurs within the time t is given by

$$P_i(t) = R_i \exp(-R_i t), \tag{1}$$

where R_i denotes the sought-after mean transition rate. To corroborate that the measured conductance fluctuations may indeed be described by a Markov process, Fig. 3 shows the good agreement between experimental (symbols) and calculated (line) integrated probability, $\int_0^t P_i(\tilde{t})\mathrm{d}\tilde{t}$. The experimental data have been obtained by statistically evaluating residence times of a given time series, i.e., by calculating the probability with which residence times, τ_i, lower than a given time, t, occur. To approximate the mean transition rate we resorted to the reciprocal mean residence time, i.e., $R_{i,\mathrm{exp}}=1/\bar{\tau}_i$, where $\bar{\tau}_i$ denotes the arithmetic mean residence time as calculated from measured times series of conductance fluctuations. However, due to the finite time resolution of the experimental setup, arbitrarily small residence times cannot be resolved and thus do not enter in the calculation of $\bar{\tau}_i$. As a consequence, the mean residence time $\bar{\tau}_i$ contains a small systematic error and $R_{i,\mathrm{exp}}$ deviates from the ideal R_i. To estimate this deviation, the inset in Fig. 3 shows the ratio $R_{i,\mathrm{exp}}/R_i$ as a function of R_i. For fluctuation rates R_i below

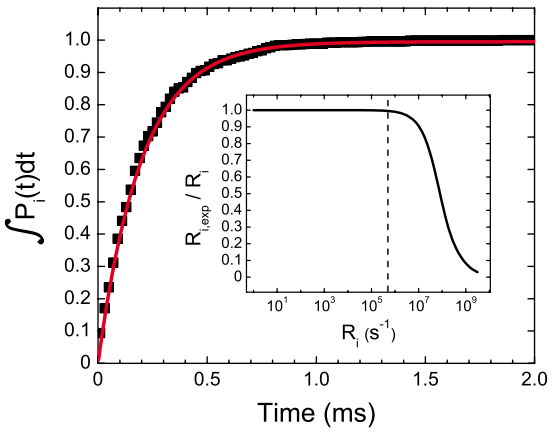

FIG. 3. (Color online) Integrated probability for a typical time series of conductance fluctuations at the fcc adsorption site measured at a sample voltage of −0.3 V. Experimental data appear as symbols while the line represents a fit to experimental data according to $\int_0^t P_i(\bar{t})d\bar{t}$ with P_i from Eq. (1). Inset: Ratio of the mean fluctuation rate $R_{i,\mathrm{exp}}=1/\bar{\tau}_i$ as extracted from the arithmetic mean residence time $\bar{\tau}_i$ and the expected transition rate R_i [Eq. (1)] as a function of R_i. The dashed line denotes the maximum fluctuation rate of 5×10^5 s^{-1} as measured in the experiments.

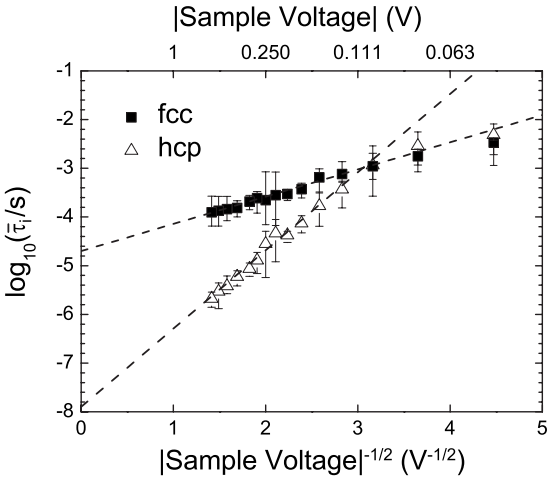

FIG. 4. Logarithm of the residence time $\bar{\tau}_i$ (i=hcp: △, i=fcc: ■) as a function of $|V|^{-1/2}$ for a representative fluctuation measurement. Dashed lines are fits to data for $|V|>0.1$ V according to Eqs. (2) and (3).

5×10^5 s^{-1}, which is the highest rate observed in the experiments reported here, the deviation of $R_{i,\mathrm{exp}}$ from R_i is less than 0.5%. As a consequence, the arithmetic mean residence time describes the real mean residence time very well.

To describe the experimental observations, we assume that the conductance fluctuations are induced by lateral translations of the adatom, which may be facilitated by a lowering of the diffusion barrier height between adjacent adsorption sites owing to the presence of the tip.[11] These translations are most likely due to adatom vibrations excited by inelastically tunneling electrons. The dynamics of such lateral adatom translations may be described by an Arrhenius-type expression for the average time of the adatom in adsorption site i,

$$\bar{\tau}_i = \tau_{0,i}\exp\left(\frac{E_i-\zeta_i V}{k_B T_{\mathrm{eff},i}}\right), \tag{2}$$

where $\tau_{0,i}$ is the attempt time, E_i the diffusion barrier height separating fcc and hcp sites in the presence of the tip, ζ_i is the electromigration parameter, which takes a possible asymmetry for positive and negative voltages into account,[7,8] k_B is Boltzmann's constant, and $T_{\mathrm{eff},i}$ is the effective temperature of the adatom. The voltage dependence of the effective temperature has been derived by Todorov,[18,19] who explicitly considered heat transfer into the electrodes,

$$T_{\mathrm{eff},i} = \sqrt[4]{T_0^4+\alpha_i^4 V^2}. \tag{3}$$

Here, T_0 denotes the ambient temperature and α_i describes the dependence of $T_{\mathrm{eff},i}$ on the voltage. This expression for the effective temperature is consistent with several experimental results.[3,20–22]

In experiments with positive and negative voltages, we found no significant influence of the voltage polarity on the mean occupation times, which indicated a small electromigration parameter. Indeed, fits to experimental data presented in Fig. 4 worsened appreciably for $|\zeta_i|>0.005$ eV/V. As a consequence, ζ_i was neglected in the subsequent analysis.

In Fig. 4 the logarithms of the average residence times at fcc (squares) and hcp (triangles) sites are plotted as a function of the sample voltage. While for $|V|<0.1$ V these times are similar, for $|V|>0.1$ V the average time the adatom resides at the hcp site becomes lower than the average time at the fcc site. The overall evolution of the average occupation time with the voltage is well described by Eqs. (2) and (3). The dashed lines in Fig. 4 are fits to experimental data according to these equations with $T_{\mathrm{eff},i}=\alpha_i\sqrt{|V|}$ for $|V|>0.1$ V (hcp) and $|V|>0.15$ V (fcc). For these voltages the term T_0^4 in Eq. (3) may be neglected compared to $\alpha_i^4V^2$. Deviations of the fits from experimental data were observed for $|V|<0.1$ V, which can be explained by the ambient temperature, T_0, which becomes more important for smaller voltages. Averaging the intersections of the fits with the ordinate for all investigated adatoms, we obtained that $\tau_{0,\mathrm{fcc}}$ ($\tau_{0,\mathrm{hcp}}$) varied between $10^{-4.8}$ and $10^{-3.8}$ s ($10^{-8.2}$ and $10^{-6.5}$ s). These values are remarkably high compared to typical attempt times reported for self-diffusion of Ag adatoms on Ag(111), which range between 10^{-12} and 10^{-11} s.[23] However, Boisvert *et al.*[24] showed that the attempt time depends on the diffusion barrier height, which separates the adjacent adsorption sites. In particular, with decreasing barrier height the attempt time may increase by several orders of magnitude. High values of the attempt time have been predicted for CO on Cu(110) by helium atom scattering[25] and then confirmed by STM experiments.[26] Tunneling from thermally excited states of CO has been suggested to be the reason for extraordinarily high attempt times for CO diffusion on Cu(111).[27] A theoretical treatment of diffusion processes on metal surfaces[28] demonstrated that neglecting adsorbate-adsorbate interactions may be at the origin of diffusion prefactor anomalies that have been extracted from nucleation experiments.[29–31] As we will show below, the presence of the tip and its attractive interaction with the adatom lowers diffusion barrier heights appreciably and thus may be the reason for the high attempt times.

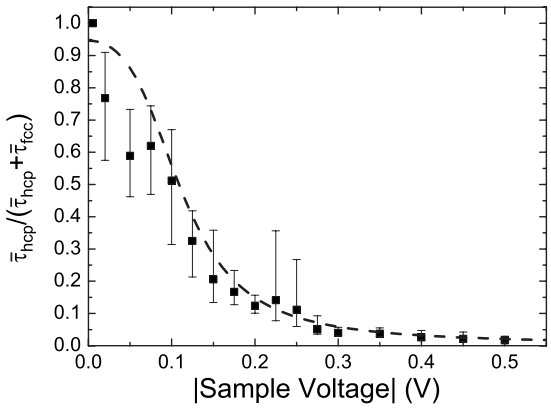

FIG. 5. Duty cycle for the adatom of Fig. 3 as a function of the voltage. The dashed line depicts simulated data based on Eqs. (2) and (3) and fit parameters summarized in Table I.

The fit of experimental residence times has been performed neglecting the ambient temperature, T_0, and led to the attempt times $\tau_{0,i}$ and the slopes E_i/α_i of the dashed lines in the Arrhenius-type plot of Fig. 4. To determine the diffusion barrier heights E_i and the parameters α_i, the so-called duty cycle, $\bar{\tau}_{hcp}/(\bar{\tau}_{hcp}+\bar{\tau}_{fcc})$,[7] was fitted using Eqs. (2) and (3) taking into account T_0. Figure 5 shows the evolution of the duty cycle as a function of the sample voltage. For high voltages, it approaches zero, which means that the hcp site is visited very briefly by the adatom and that the fcc site is preferentially occupied. Starting from $|V| \approx 0.1$ V, where $\bar{\tau}_{hcp}/(\bar{\tau}_{hcp}+\bar{\tau}_{fcc})$ is approximately 50%, this trend is inversed for $|V| < 0.1$ V and the hcp site becomes the preferred site, i.e., the adatom is located near the tip apex. For nearly zero voltages the duty cycle reaches values close to 100% reflecting the adatom staying at the hcp site close to the tip apex. This observation is in agreement with molecular-dynamics simulations of tip-induced lateral atom manipulation at zero voltage.[32] In the absence of an applied voltage between tip and sample Yildirim *et al.*[32] showed that Ag (Cu) adatoms on Ag(111) [Cu(111)] follow the lateral trajectory of the tip apex. Using Eqs. (2) and (3) the behavior of the duty cycle was simulated (dashed line in Fig. 5). With $\zeta_i=0$, $T_0=7$ K and the ratio E_i/α_i extracted from the slopes of the fits in Fig. 4, only two fit parameters were left to describe the voltage dependence of the duty cycle. In Table I the fit parameters obtained for three investigated atoms are compared.

Remarkably, the barrier height between the adsorption sites is several millivolts only, which is much less than the reported diffusion barrier height for Ag adatoms on Ag(111) ($\approx$100 meV).[23] Most likely, the observed lowering of the barrier height is due to the presence of the tip, as proposed in Ref. 11. Adatom translations in the combined potential of tip and surface have also been reported in Ref. 33. When the tip is positioned above a bridge position between hcp and fcc sites [Fig. 1(a)], the barrier height is substantially lowered owing to the superimposed tip potential.[11] As a consequence of the strongly lowered barrier heights we access an extraordinary imaging mode, which porvides atomic resolution. The STM image in Fig. 6 was acquired by dragging a Ag adatom with the scanning tip. During the measurement the adatom follows the tip by hopping from fcc to hcp sites. Similar

TABLE I. Summary of fit parameters obtained from two-level fluctuations of three adatoms. Adatom 1 was analyzed at positive sample voltage, while Adatoms 2 and 3 were investigated at negative voltages.

Adatom	Polarity	i	$\log(\tau_{0,i}/\mathrm{s})$	E_i (meV)	α_i (K/$\sqrt{\mathrm{V}}$)
1	+	fcc	−4.8	1	20.5
		hcp	−8.2	11.3	37.1
2	−	fcc	−4.7	1.8	19.9
		hcp	−7.9	8.1	25.4
3	−	fcc	−3.8	1.4	19.9
		hcp	−6.5	6.6	30.1

tip-induced adatom translations have been reported for, e.g., quantum corral construction using single atoms[15] and single-atom manipulation on vicinal surfaces.[34] Bright areas in Fig. 6 correspond to fcc and hcp sites, where the adatom prefers to stay close to the tip at the chosen tunneling parameters (0.1 V, 2 μA). Dark areas monitor sites, which for the adatom are energetically not favorable (bridge and top sites) and which thus lead to an increase in the tip-adatom distance. The tip is accordingly moved closer to the surface giving rise to the depressions in the constant-current STM image. In contrast to a similarly acquired STM image using a dragged Co adatom on Cu(111) where Cu(111) fcc sites appeared larger than hcp sites,[11] fcc and hcp sites appear with virtually identical lateral dimensions on Ag(111) when imaged with a dragged Ag adatom. In an additional experiment, which is not discussed in detail here, we imaged a Cu(111) surface with a dragged Cu adatom and obtained a similar difference in the lateral dimensions of fcc and hcp sites as observed for Co on Cu(111).[11] These observations may tentatively be explained on the basis of different adsorption energies in fcc and hcp sites for Cu(111) and Ag(111). The experimental observations on Cu(111) are compatible with a higher adsorption energy at the fcc than at the hcp site. In this case, the tip has to be close to the hcp site until the deformation of the hcp potential due to the tip is strong enough to make the adatom hop from the fcc to the hcp site. In contrast, ap-

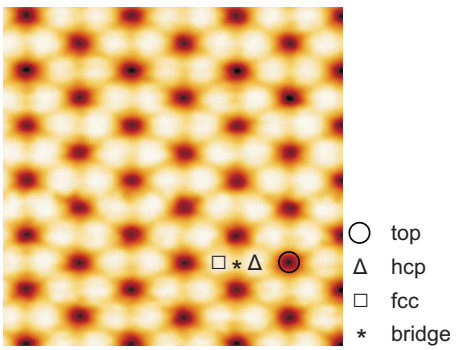

FIG. 6. (Color online) Constant-current STM image of Ag(111), which was obtained by dragging a single Ag adatom. Dark areas correspond to top (circle) and bridge (asterisk) sites, while bright areas are fcc and hcp sites (square and triangle) 1.7 nm × 1.7 nm, 0.1 V, and 2 μA.

proaching a fcc site a slight deformation of the fcc adsorption potential is necessary to drag the adatom from the hcp to the fcc site. Consequently, hcp sites appear with smaller lateral dimensions than fcc sites on Cu(111). For Ag(111) the difference between fcc and hcp adsorption potentials appears to be marginal, which results in the observed essentially identical dimension of fcc and hcp sites during imaging.

According to Table I, for all investigated adatoms the barrier heights E_{fcc} and E_{hcp} differ by factors of 5 to 10. In particular, the energy needed to induce a transition from fcc to hcp is smaller than for the inverse transition. This observation may be understood by the presence of the tip, which in the experiments is positioned closer to the hcp than to the fcc site. According to a theoretical investigation, the adatom exhibits the propensity to stay close to the tip apex atom at zero voltage,[32] which is in good agreement with a duty cycle of ≈100% at very low voltages (Fig. 5). Higher voltages provide higher energies to the tunneling electrons, which excite adatom translations to the adjacent fcc site. Despite these translations the adatom prefers to stay close to the tip, which explains the different barrier heights. This phenomenon is closely related to the different heating of the adatom in hcp and fcc sites. According to Table I, the parameter α_i is always higher for hcp than for fcc sites, which is due to the closer proximity of the adatom to the tip at the hcp site, which in turn is related to a higher current across the adatom. By simulating effective temperatures of Ag adatoms according to Eq. (3) and to the obtained fitting parameters (Table I), we found that local heating at the hcp site is more pronounced than at the fcc site (Fig. 7). At 0.5 V, for instance, the effective temperature of the adatom at the hcp site is ≈18 K, while it is ≈14 K at the fcc site. Compared to effective temperatures of several hundreds of Kelvin reported for single-molecule junctions,[3–5,35] the adatom effective temperatures are low. A possible reason for this difference may be the low decay rate of molecule vibrations due to an inefficient coupling with the phonon modes of the electrodes.[36] A low decay rate can result from a mismatch of vibrational density of states of the molecule and the electrodes. For instance, 174 out of a total of 180 vibration modes of C_{60} exhibit energies exceeding 25 meV and are thus higher than typical metal phonon energies.[37] Further reasons for low decay rates of molecular vibrational excitations into the phonon bath of the electrodes may be due to the vibration modes located far from the electrodes[36] or due to molecular orbitals that carry the electron flow and provide an enhanced electron-vibration coupling.[5,36] The single metal adatom, however, exhibits vibrational energies[38] that match the phonon energies of the electrodes. As a consequence, heat dissipation to the substrate is more effective for the adatom than for the molecule, which may explain the lower effective temperature of the adatom.

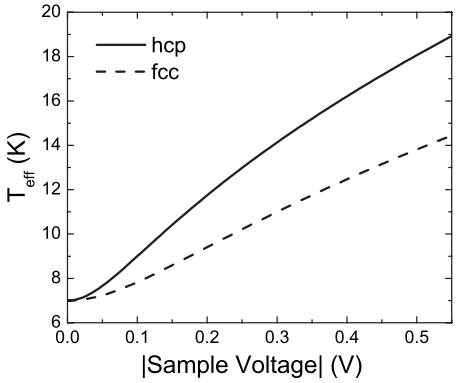

FIG. 7. Simulated effective temperatures of Ag adatom residing at hcp (solid line) and fcc (dashed line) sites of Ag(111). Calculations are based on Eq. (3) and fit parameters for Adatom 2 (Table I).

IV. CONCLUSION

Lateral translations of a Ag adatom on Ag(111) between adjacent adsorption sites were monitored by time-resolved two-level conductance fluctuations of the tunnel junction. The presence of the tip considerably lowers the diffusion barrier heights of the adatom and leads to different heating of the adatom depending on its relative position to the tip. From the voltage dependence of conductance fluctuation rates the temperature of the junction has been estimated.

ACKNOWLEDGMENTS

Discussions with E. Pehlke (University of Kiel) and funding by the Deutsche Forschungsgemeinschaft through SPP 1153 are acknowledged.

*kroeger@physik.uni-kiel.de

[1] D. G. Cahill, W. K. Ford, K. E. Goodson, G. D. Mahan, A. Majumdar, H. J. Maris, R. Merlin, and S. R. Phillpot, J. Appl. Phys. **93**, 793 (2003).
[2] A. Pecchia, G. Romano, and A. Di Carlo, Phys. Rev. B **75**, 035401 (2007).
[3] Z. Huang, B. Xu, Y. Chen, M. Di Ventra, and N. Tao, Nano Lett. **6**, 1240 (2006).
[4] N. Néel, J. Kröger, L. Limot, T. Frederiksen, M. Brandbyge, and R. Berndt, Phys. Rev. Lett. **98**, 065502 (2007).
[5] G. Schulze, K. J. Franke, A. Gagliardi, G. Romano, C. S. Lin, A. L. Rosa, T. A. Niehaus, Th. Frauenheim, A. Di Carlo, A. Pecchia, and J. I. Pascual, Phys. Rev. Lett. **100**, 136801 (2008).
[6] K. S. Ralls and R. A. Buhrman, Phys. Rev. Lett. **60**, 2434 (1988).
[7] K. S. Ralls, D. C. Ralph, and R. A. Buhrman, Phys. Rev. B **40**, 11561 (1989).
[8] P. A. M. Holweg, J. Caro, A. H. Verbruggen, and S. Radelaar, Phys. Rev. B **45**, 9311 (1992).
[9] H. E. van den Brom, A. I. Yanson, and J. M. van Ruitenbeek, Physica B **252**, 69 (1998).
[10] N. Agraït, J. G. Rodrigo, and S. Vieira, Phys. Rev. B **47**, 12345 (1993).
[11] J. A. Stroscio and R. J. Celotta, Science **306**, 242 (2004).

[12] L. Limot, J. Kröger, R. Berndt, A. Garcia-Lekue, and W. A. Hofer, Phys. Rev. Lett. **94**, 126102 (2005).
[13] A. Sperl, J. Kröger, N. Néel, H. Jensen, R. Berndt, A. Franke, and E. Pehlke, Phys. Rev. B **77**, 085422 (2008).
[14] J. Kröger, N. Néel, and L. Limot, J. Phys.: Condens. Matter **20**, 223001 (2008).
[15] CS.-W. Hla, K.-F. Braun, and K.-H. Rieder, Phys. Rev. B **67**, 201402(R) (2003).
[16] D. M. Eigler and E. K. Schweizer, Nature (London) **344**, 524 (1990).
[17] S.-W. Hla, J. Vac. Sci. Technol. B **23**, 1351 (2005).
[18] T. N. Todorov, Philos. Mag. B **77**, 965 (1998).
[19] T. N. Todorov, J. Hoekstra, and A. P. Sutton, Phys. Rev. Lett. **86**, 3606 (2001).
[20] R. H. M. Smit, C. Untiedt, and J. M. van Ruitenbeek, Nanotechnology **15**, S472 (2004).
[21] M. Tsutsui, Y. Teramae, S. Kurokawa, and A. Sakai, Appl. Surf. Sci. **252**, 8677 (2006).
[22] M. Tsutsui, S. Kurokawa, and A. Sakai, Appl. Phys. Lett. **90**, 133121 (2007).
[23] H. Brune, Surf. Sci. Rep. **31**, 121 (1998).
[24] G. Boisvert, L. J. Lewis, and A. Yelon, Phys. Rev. Lett. **75**, 469 (1995).
[25] M. F. Bertino, F. Hofmann, W. Steinhögl, and J. P. Toennies, J. Chem. Phys. **105**, 11297 (1996).
[26] B. G. Briner, M. Doering, H.-P. Rust, and A. M. Bradshaw, Science **278**, 257 (1997).
[27] A. J. Heinrich, C. P. Lutz, J. A. Gupta, and D. M. Eigler, Science **298**, 1381 (2002).
[28] S. Ovesson, A. Bogicevic, G. Wahnström, and B. I. Lundqvist, Phys. Rev. B **64**, 125423 (2001).
[29] J. V. Barth, H. Brune, B. Fischer, J. Weckesser, and K. Kern, Phys. Rev. Lett. **84**, 1732 (2000).
[30] H. Brune, K. Bromann, H. Röder, K. Kern, J. Jacobsen, P. Stoltze, K. Jacobsen, and J. Nørskov, Phys. Rev. B **52**, R14380 (1995).
[31] B. Fischer, H. Brune, J. V. Barth, A. Fricke, and K. Kern, Phys. Rev. Lett. **82**, 1732 (1999).
[32] H. Yildirim, A. Kara, and T. S. Rahman, Phys. Rev. B **75**, 205409 (2007).
[33] A. Kühnle, G. Meyer, S. W. Hla, and K.-H. Rieder, Surf. Sci. **499**, 15 (2002).
[34] L. Bartels, G. Meyer, and K.-H. Rieder, Phys. Rev. Lett. **79**, 697 (1997).
[35] Y. C. Chen, M. Zwolak, and M. Di Ventra, Nano Lett. **3**, 1691 (2003).
[36] G. Romano, A. Pecchia, and A. Di Carlo, J. Phys.: Condens. Matter **19**, 215207 (2007).
[37] J. Kröger, Rep. Prog. Phys. **69**, 899 (2006).
[38] S. D. Borisova, S. V. Eremeev, G. G. Rusina, V. S. Stepanyuk, P. Bruno, and E. V. Chulkov, Phys. Rev. B **78**, 075428 (2008).